Nigerian Journal of Physics (NJP)
ISSN online: 3027-0936
ISSN print: 1595-0611
DOI: 4https://doi.org/10.62292/njp.v33i3.2024.296
Volume 33(3), September 2024

Classification of Shallow Subsurface Heterogeneity, using 2-D Wenner Array and Induced Polarization Methods, in Parts of Southern Ijaw, Bayelsa State, Nigeria

[1]Adedokun, I. O. and [2]Etim, D. U.

[1]Niger Delta University, Wilberforce Island, Bayelsa State, Nigeria.
[2]Rivers State University, Port Harcourt, Rivers State, Nigeria.

*Corresponding author's email: ioadedokun@yahoo.com

ABSTRACT

An integrated study, consisting of 2-D Wenner array and Induced Polarization (IP) measured at five profiles, were used to characterize the near surface heterogeneity in Southern Ijaw area of Bayelsa State. Using Abem Terrameter (SAS 1000) for both measurements, five 2-D resistivity profile lines with electrode spacing of 5.00m and electrode spread of 100.00m were employed. Computer software, RES2DINV was adopted for the interpretation of the data while Microsoft Excel software was used for plotting the IP chargeability anomaly against electrode distance. The results showed various resistivity distributions with the lowest value of 1.98Ωm and highest value 638Ωm indicating fine Clay and medium coarse sand respectively. The resistivity varies horizontally and vertically, and such that at the base it is higher than that of the topsoil except in profiles 3 and 5. Resistivity ranges for the profiles are profile 1 (5.96-175Ωm), profile 2 (1.98-495Ωm), profile 3 (46.5-638Ωm), profile 4 (20.3-187Ωm) and profile 5 (10.1-485Ωm). Positive and negative Induced Polarization (IP) chargeability were recorded in all the profiles. However, at Profile 1(NDU New site), negative IP effect was encountered throughout with range values between 0 and -450ms chargeability. This result is associated with the distribution of chargeable zones in the ground and also due to a thin chargeable layer at the surface. Few measurable negative values were also recorded at Profiles 2, 3, 4 and 5. Positive IP values were encountered in greater part of the profiles: profile 2 (0 – 80ms) profile 3 (0-3ms) profile 4 (0- 3ms) and profile 5(0-8ms). The signatures obtained from the IP effects are indicators of Clay sediment of various compositions which corroborate with, to a reasonable extent, the observation from the inverse 2-D resistivity section. The sediments observed in the study area can be classified into clay, clayey sand, fine clayey sand and medium sand. The result of this research will contribute immensely to the infrastructural development of the rapidly expanding community in this area.

Keywords:
Induced Polarization,
Resistivity,
RES2DINV,
Abem Terrameter.

INTRODUCTION

In every attempt to develop the infrastructure of the community or town, ground is involved and plays significant roles in this regard. Therefore adequate knowledge of what is under the surface, its nature and attributes or properties are necessary. As people move to this area where the State's University is located, they construct more buildings, tap into the underground water, go into farming, and other human activities that have direct bearing on the subsurface and thus make the knowledge of the subsurface sediments desirable, if not compulsory. The study has shown that IP imaging is a promising tool for mapping lithological contrasts in unconsolidated sediments and to clarify difficulties in lithological interpretation observed in other geophysical methods (Alabi et al., 2010). However, it is desirable to have better results when two geophysical methods complement each other. In order to achieve this objective, two geophysical methods have been combined to characterize and identify the lithologic units near the surface (Aizebeokhai et al., 2016) in the study area. These are 2-D Wenner array and Induced Polarization (IP) methods.

Electrical properties are among the most useful geophysical parameters in characterizing earth materials as the variations in electrical resistivity (or conductivity)

typically correlate with variations in lithology, water saturation, fluid conductivity, porosity and permeability (Van Schoor, 2002). Resistivity method is widely used in geophysical prospecting, such as hydro-geological (TerraDat, 2005; Chambers et al., 2006; Chang, et al., 2017), geological structure (Zhang et al., 2016), engineering Caputo et al., 2003) and environmental surveys (Arjwech et al., 2019). The resistivity value of rocks and minerals depend on geology and the structure of the minerals but have no specific values but specific range (LAYADE ET AL., 2017).

Resistivity and chargeability are popular geophysical methods which are being applied to mineral exploration and, in environmental studies, are often used to delineate contaminant plumes and geological boundaries (Aristodemou & Thomas-Betts, 2000). According to Johansson (Johansson, 2007) the combination of resistivity and time domain induced polarization (IP) can improve the use of and effectiveness of the geoelectrical methods. The use of non-invasive surface geophysical techniques is of great relevance in that reasonably factual subsurface information is obtained without any destruction to the environment within a relatively short time. Electrical resistivity and time domain induced polarization have shown to be of good complementary in this regard. The geoelectrical method provides a wide range of variations in the subsurface electrical resistivity. These variations are often associated with water content and lithology; hence, it is one of the most powerful geophysical methods often used in providing solutions to hydrogeological problems (Chambers et al., 2006; Zhang et al., 2016; Zhang et al., 2016). Actually, no work has been done in this area to know and characterize the subsurface strata. Consequently, this study was carried out to know the near-surface geologic setting, identified the formations and their depths, for the benefits of growing population within the study area

Location and geology of the study area

The study area (Figure 1), Southern Ijaw is in Bayelsa State, located within Latitudes (4^0 55'N – 5^0 1'N) and Longitudes (6^0 4'E-6^0 14'E) in Niger Delta, Nigeria. The study area lies within Tropical rain forest climate characterized by rainy season and short dry season. It is drained by tributaries from River Nun and has an average rainfall and temperature of 2,899 mm and 26.7 ^{0}C respectively. As expected the major socio-economic activities of the people in the area are fishing and farming. Its mean elevation is about 8 m above the mean sea level. The geologic sequence of the Niger Delta consists of three main tertiary subsurface lithographic units (Benin, Agbada and Akata Formations) which are overlain by various types of quaternary deposit (Short & Stauble, 1967)

The topmost unit is the Benin Formation which comprises of over ninety percent sandstone with shale intercalations. It is coarse grained gravely, locally fine grained, poorly sorted, sub-angular to well-rounded and bears lignite streaks and wood fragments. The unit is thickest in the central area of the Delta. Its contact with the underlain Agbada Formation is defined by the base of Sandstone which also corresponds to the base of the fresh water bearing strata (Allen, 1965). The sandstones in the Agbada Formation are generally well-sorted, moderately well-rounded, and have high porosity and permeability, making them important aquifers in the area (Ganiyu et al., 2015). The shales in the formation, on the other hand, act as confining units that separate the aquifer zones and restrict the movement of groundwater. The thickness of the shale layers can greatly affect the hydraulic conductivity of the aquifers, as they provide a barrier to vertical flow (Koda et al., 2017). The Akata Formation, an important source of rock for hydrocarbons, is a sequence of dark, organic-rich shales that underlies the Agbada Formation. It was deposited during the Late Cretaceous and Early Tertiary periods and is part of the sedimentary succession of the Niger Delta Basin (Nwajide, 2013).

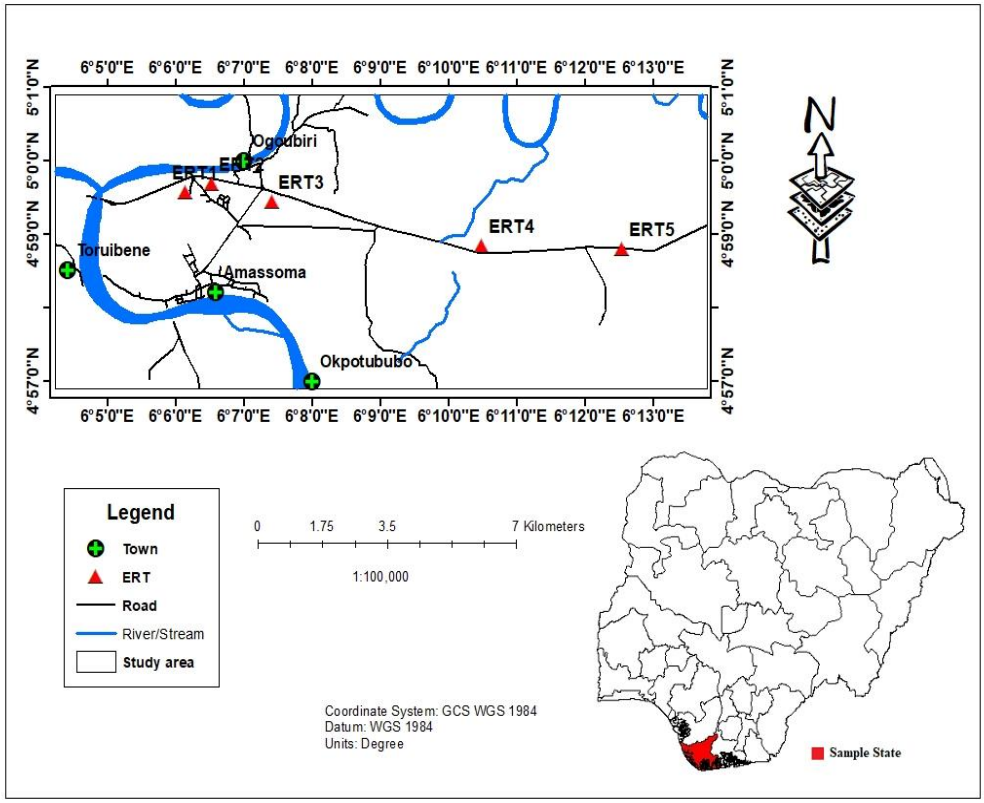

Figure 1: Location map showing the study area and its environs

MATERIALS AND METHODS

Abem (SAS1000) Terrameter was used for both 2-D Wenner array survey and Induced Polarization measurement (IP). Time-domain IP method depends on a small amount of electric charge being stored in the ground when a current is passed through it, to be released and measured when the current is switched off. When a direct current is passed into the ground the magnitude of the Induced polarization IP observed is expressed as

$$\frac{\Delta V}{V} \qquad (1)$$

where $\Delta V$is the voltage remaining at a definite time, t_1 tot_2, after the current is cut off. The normalized time integral, called the Chargeability, measured in millivolt second per volt or millisecond, is given as (Parasnins, 1986)

$$\frac{1}{V}\int_{t_1}^{t_2}\Delta V dt \qquad (2)$$

For the 2-DWenner array, the apparent resistivity ρ_a is calculated from the product of resistivity R recorded and the geometric factor k where 'a' is the electrode spacing

$$\rho_a = 2\pi a\frac{\Delta V}{I} = \frac{\Delta V}{I}k = Rk \qquad (3)$$

k is the geometric factor which depends entirely on the type of array employed and resistance R represents the reading displays by the resistivity equipment (Telford et al., 1990).

The measurements were carried out concurrently with the equipment along the five profiles, each 100.00m in length. After the 2-D reading was taken, the field of measurement on the equipment was switched to IP mode and the reading recorded. Each reading was taken after necessary precautions, such as good electrode contact with the ground, survey conducted along a straight line and away from cultural features. Checking for current leakage and creeps to avoid spurious measurements were also observed (Abdullah, 2018). The 2-D Wenner measurement commenced with electrode spacing of 5, 10, 15,20, 25, 30, 35, … for each sequence on electrode spread of 100.00m which was completed before taking the next profile (Dahlin, & Loke, 1998). For each electrode spacing interval, readings of 2-D and IP data were taken for the profile length of 100m. This was done for the specified intervals for all the five profiles covered. The computer software program, RES2DINV, was used for the 2-D data inversion to yield Figures (3,5,7,9 and 11). Similarly, excel software program was used for the plotting the IP chargeability values, in milliseconds, against the electrode distance in metre, to obtain the anomalies in Figures (4, 6, 8, 10 and 12).

RESULTS AND DISCUSSION

Figures 2,4,6,8 and 10 show the 2-D resistivity inversion while Figures (3,5,7, 9 and 11) represent the anomalies of the Induced Polarization (IP) chargeability. The results of the 2-D resistivity inversion are presented in this order: (Resistivity, Depth, Spread along the profile). At the Profile 1 (Ndu New Site),the topsoil resistivity ranges between45.3 and 89.1 Ωm for most part and 89.1 to 175 Ωm for a few meters at the beginning of the profile. The percolation of rain water from the surface gives rise to a much lower resistivity in the subsoil. From Figure 2, (Resistivity:90Ωm, Depth:1.25-15.9m, Spread:7-100m). The formation could be clayey sand. It exists throughout the entire profile with different thicknesses as indicated: (Resistivity:175Ωm, Depth:1.25-19.8m, Spread:4-100m). The formation could be fine sand. It penetrates throughout the profile and beyond with varying thicknesses at different levels: Resistivity: 89.1Ωm, Depth:1.25-12.4m, Spread:6-100m). The formation is likely composed of sandy clay. It is present in the entire profile and also appears at the topsoil at intervals 16-32m, 38-51m, 54-68m and 86-92m: Resistivity:46Ωm, Depth:2.0-10m, Spread:13-40.0m, 45-66m). This layer could be wet clay. It envelopes portion of lower resistivity of about 23.0Ωm, which also surrounds a much lower resistivity ranging from about 3.03 to 11.7Ωm. This is likely to be wet fine clay.

Figure 3, represents the negative Chargeability signatures obtained from Induced Polarization (IP) data. This is between 0 and -450 ms chargeability for the entire length of the profile. The negative chargeability is as a result of the distribution of chargeable zones in relation to the sensitivity distribution which determines how different parts of the ground contribute to the measured apparent resistivity of a particular four electrode array. It could also be caused by a thin chargeable layer at the surface (Dahlin & Loke, 2015).

Generally, the profile shows resistivity ranging from 5.96-175Ωm. where 3.03-45.3Ωm is wet clay; 89.1Ωm is sandy clay; 175Ωm is fine sand.

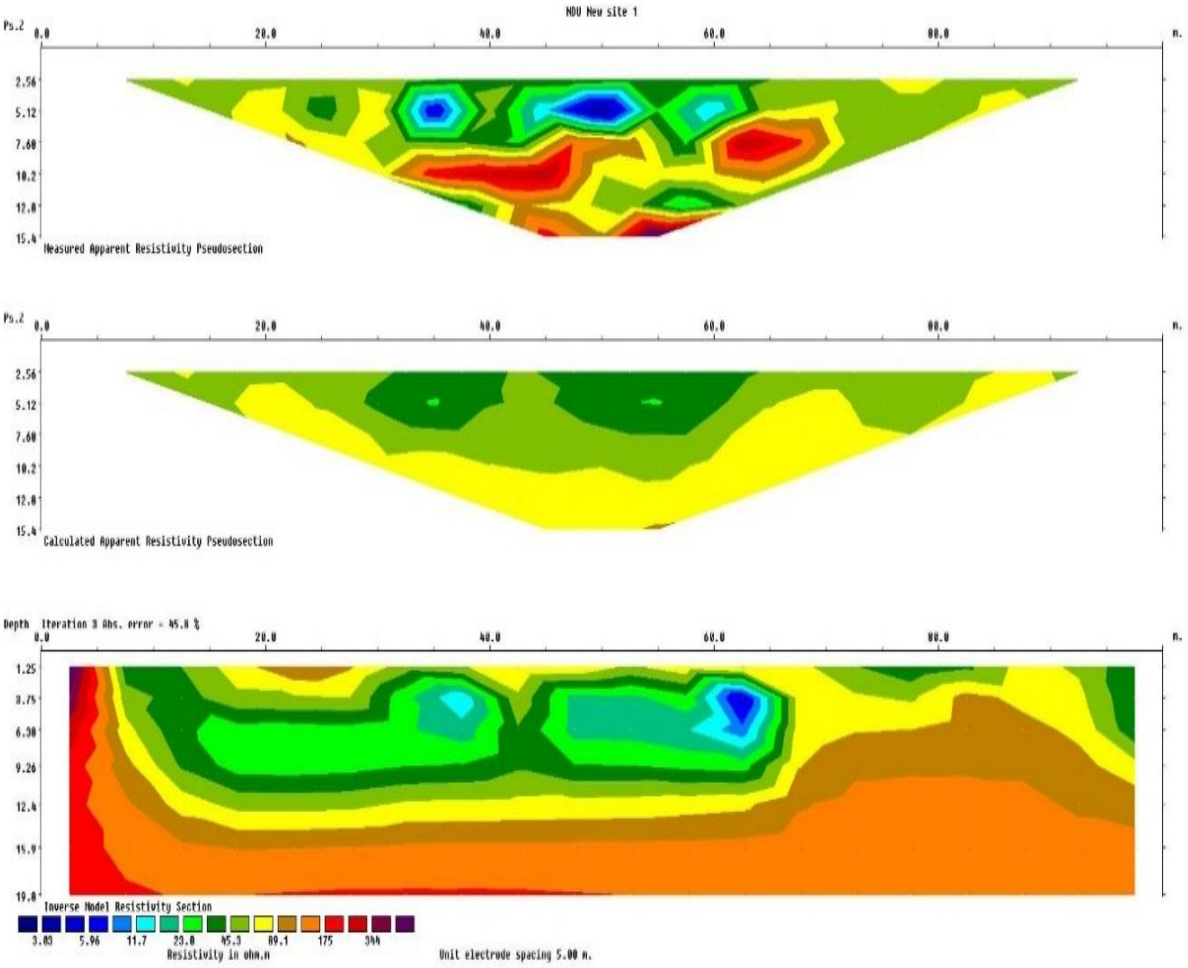

Figure 2: 2-D resistivity inversion results for profile 1

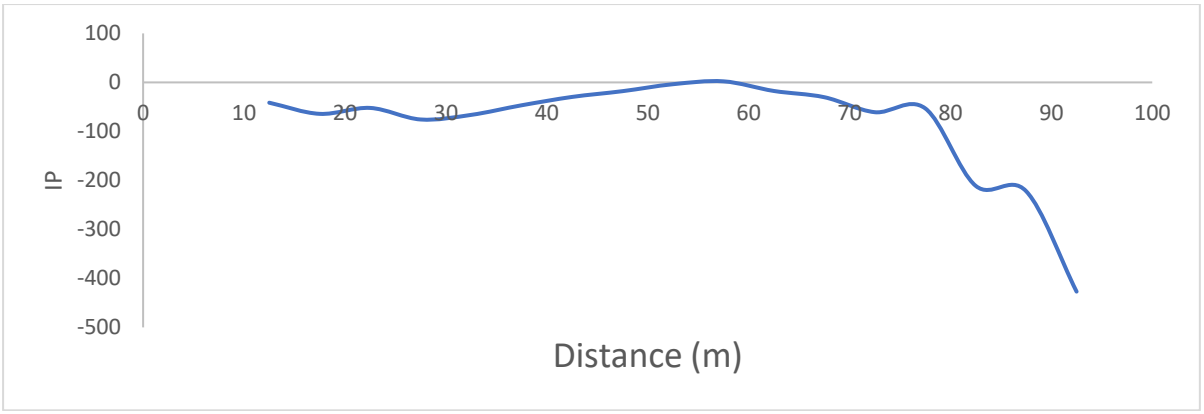

Figure 3: IP Chargeability (ms) against electrode distance X(m) for profile 1

Profile 2 (Ogobiri junction). The topsoil resistivity of this profile can be categorized into two; the wet clay (9.48-44.5 Ωm) which is underlain by a higher resistive formation (96.9 Ωm) and the dry sand (96.9-459 Ωm), which overlies layers of much lower resistivity (1.98 - 44.5 Ωm). From Figure 4, (Resistivity:96.9Ωm, Depth:2.0-19.8m and beyond, Spread:1.0-30m). The formation is likely composed of fine sandy clay. This layer exists throughout the entire profile, intruding to the surface at different distances and depths as indicated. This layer also envelopes a much higher resistive sediment of about 150Ωm which could be silt fine sand: (Resistivity:45.3Ωm, Depth:1.25-19.8m and beyond, 1.25-4.0m Spread:1-100m). This formation could be wet clay. It is observed throughout the profile at different depths and also protrudes to the surface at different distances: Resistivity: 1.98-4.32Ωm, Depth:3.75-12.4m, Spread: 55-78m). This formation is likely composed of fine wet clay enveloped by a much high resistivity ranging from 9.48-20.4Ωm. This is located between 4.0-19.8m and 48-95m distances and is likely to be wet clay: (Resistivity: 495Ωm, Depth:1.25-3.75m, Spread:54-60m). This formation in this layer is likely composed of fine medium sand.

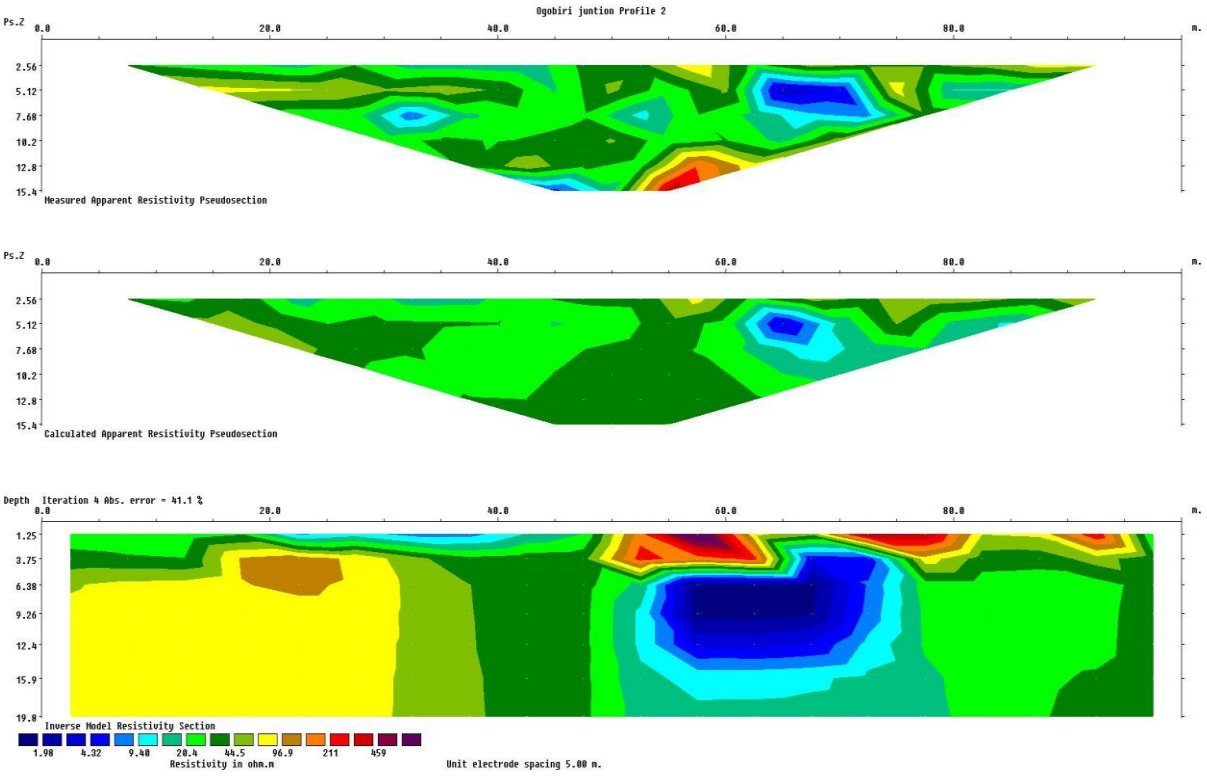

Figure 4: 2-D resistivity inversion results for profile 2

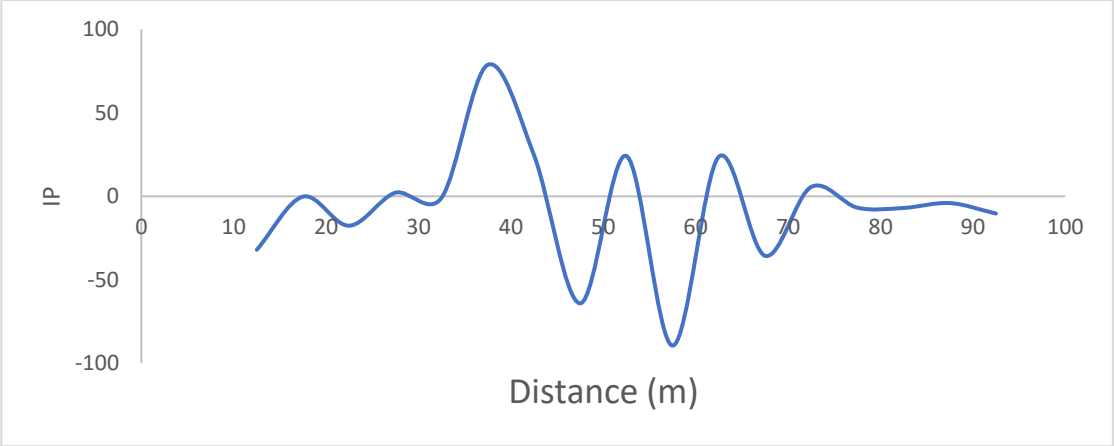

Figure 5: IP Chargeability (ms) against electrode distance X(m) for profile 2

Figure 5, the distance between 32- 43m corresponds to areas with relatively high positive Chargeability (Induced polarization IP effect) value (82 ms). It depicts accumulation of unconsolidated fine sand particle of resistivity (96.9Ωm and 211Ωm) as corroborated on the resistivity section.

As shown in Figure 4, low negative anomalies of IP were recorded at various distances along the profile indicating the distribution of chargeable zones and presence of chargeable layer at the surface. At the last depth, 19.8m, on the resistivity section, is the lowest resistivity of the profile indicating different resistivities (9.40Ωm, 20.4Ωm, 44.5Ωm) which is interpreted to be wet clay. The profile reveals resistivity ranging from 1.98-459Ωm. where 1.98-9.40 is fine wet clay; 20.0-44.5 is wet clay; 96.9 is clayey and 211-459 is fine medium sand.

From Profile 3 (Ogobiri-Tombia road), relatively higher resistivity dominates the topsoil (0 -1.25 m). Two categories can be identified: the wet clay (46.5 - 89.5 Ωm) which is underlain by much higher resistivity and medium coarse sand (172- 638 Ωm), which appears in most part of the surface and overlies the lower resistive layers underneath. From Figure 6 shows, (Resistivity: 172Ωm, Depth: 2.0-3.75m, 1.25-19.8m and beyond, Spread: 1.0-100m). This formation could be fine sand. It is present throughout the profile though having different thicknesses and also appears to the surface at different points along the profile. The next layer has (Resistivity; 638Ωm, Depth; 6.38-17.0m, Spread;15-25m). This is likely composed of medium coarse sand and is enveloped by a lower resistivity of about 311Ωm, a fine medium sand, from a depth of 4.0-19.8m and beyond, covering a distance between 9 and 27m. (Resistivity:89.5Ωm, Depth:3.75-8.0m, 5.0-19.8m and beyond, Spread:30-81m). The formation could be sandy clay. It is surrounded by a higher resistivity sandy clay of about 100Ωm between depths 2.0 and 19.8m, and beyond, extending to (28-85m) distance. Figure 8, shows small positive Chargeability IP values (1-2 ms), in most part of the profile between 29-94m indicating the presence of clay to corroborate the results on 2-D resistivity inversion of Figure 6. To a large extent, the profile shows resistivity ranging from 46.5-638Ωm. where 46.5 is wet clay; 89.5Ωm is sandy clay; 175Ωm is fine sand and 331-638Ωm is medium coarse sand.

Profile 4 (Ogobiri -Tombia road)**:** Surface resistivity is generally low ranging between 20.3 and 61.3 Ωm for a wet clayey topsoil which occupies almost the entire profile, and 107 to 187 Ωm for the dry fine sand towards the end. Like in the other profiles, generally, resistivity reverses its trends underneath. The recorded values are shown in Figure 8, (Resistivity: 61.5Ωm, Depth: 6.38-8.0m, 3.75-19.8m Spread: 1.0-100m). This portion is likely composed of clay. It exists throughout the profile and appears on the surface at a distance of about 35-36m, 40-53m, 68-71m and 86-90m though with varying thicknesses: Resistivity:20.3-35.3Ωm, Depth:1.25-14.0m, Spread:57-87m). This formation could be wet clay. (Resistivity:107Ωm, Depth:10.0-14.0m, 3.75-19.8m and beyond, Spread:1.0-62m). The formation is likely to be sandy clay. Below this layer is a much higher resistivity ranging from 150-187Ωm at a depth of 5.0-19.8m and beyond, covering a distance of 1.0-50m. This layer could be fine sand. Generally, it is a low resistivity section ranging from 3.84Ωm to 187Ωm (Figure 9). From Figure 9, low positive (Chargeability) signature of IP effect was recorded throughout the profile length except between 20 and 25m. It indicates the presence of Clay as revealed on the 2-D resistivity inversion in Figure 9. The profile, generally, shows resistivity ranging from 20.3-187Ωm where 20.3-61.5Ωm is clayey and 107-187 is fine sand.

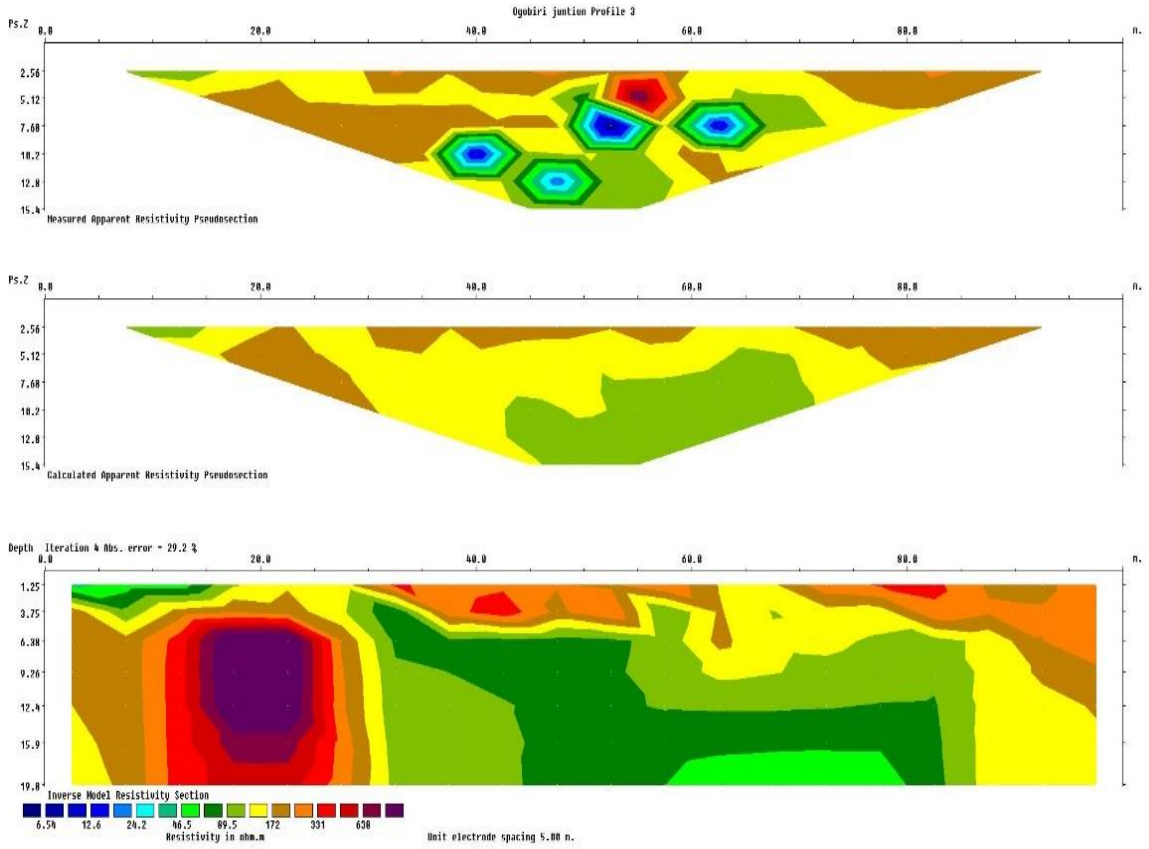

Figure 6: 2-D resistivity inversion results for profile 3

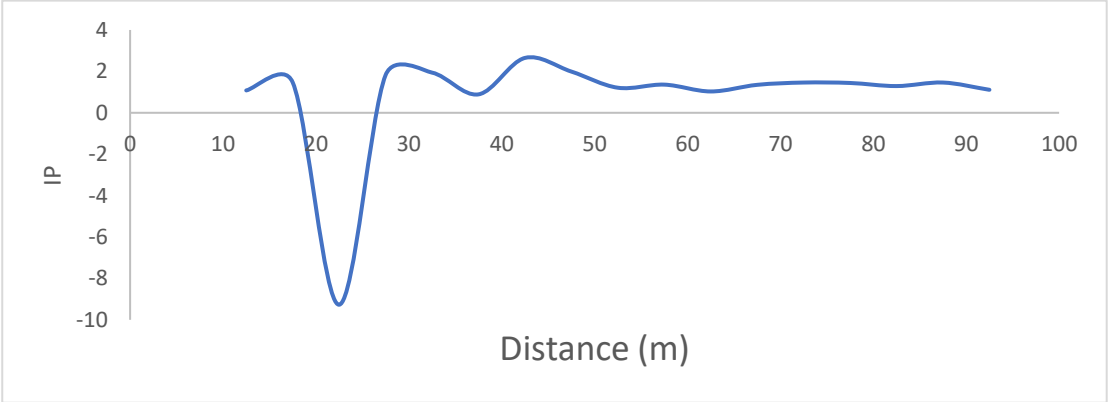

Figure 7: IP Chargeability (ms) against electrode distance X(m) for profile 3

Profile 5 Airport road is where two resistivity values range define the topsoil of this profile; between 18.1and 69.9Ωm which represents wet clay and stretches almost throughout the entire profile, and a fractional portion of fine sand (184 Ωm) sandwiched at the surface. Unlike the previous profiles, the layers continue downward beyond the depth covered in this work and are more or less at angles to the horizontal.

Figure 10, (Resistivity: 184Ωm, Depth:10.0-14.0m, 7.0-19.8m and beyond, Spread:1.0-16m). The formation is likely composed of fine sand with different thicknesses at different depths.

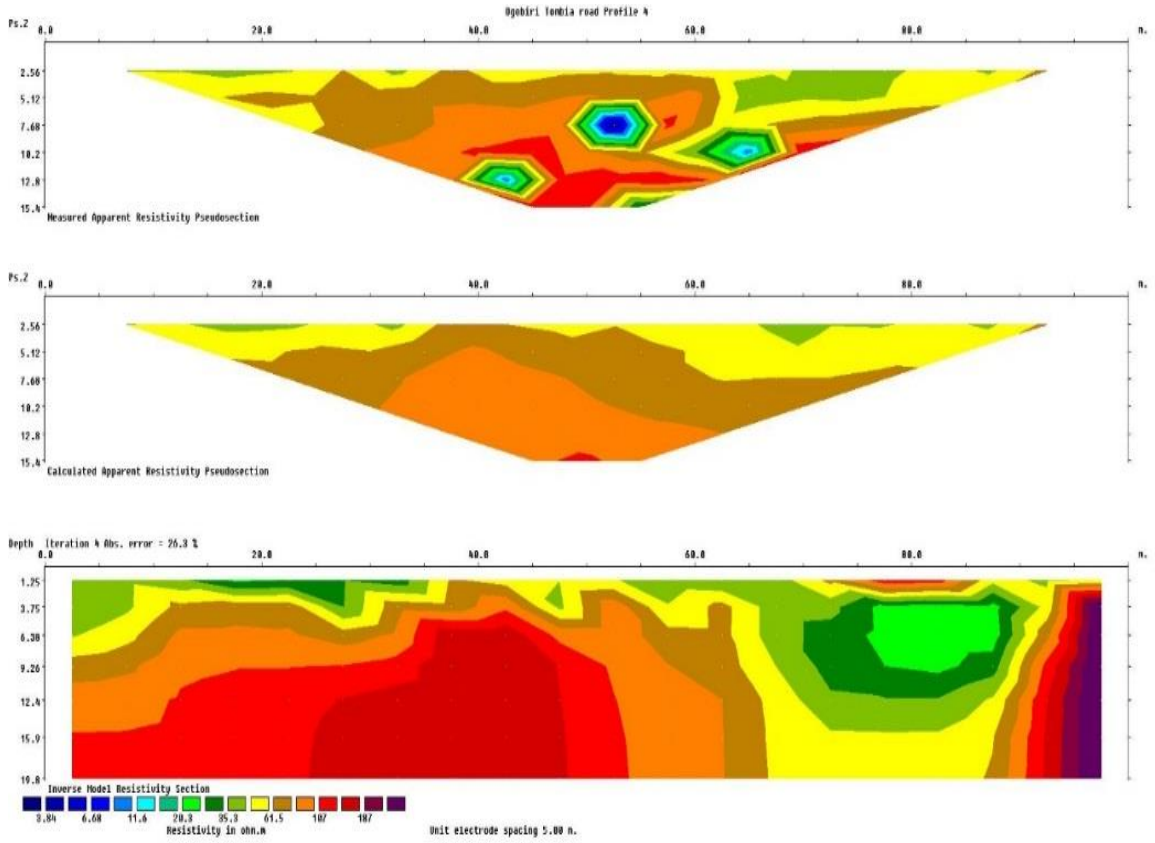

Figure 8: 2-D resistivity inversion results for profile 4

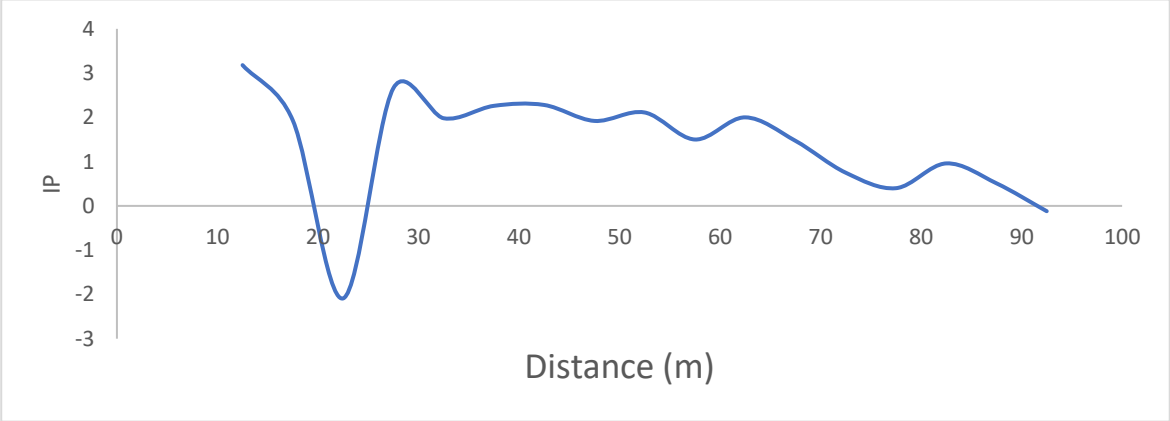

Figure 9: IP Chargeability (ms) against electrode distance X(m) for profile 4

Under this layer is a shallow resistivity of about 300Ωm at a depth of 14.0-19.8 and beyond covering a distance between 1.0-10m. This layer could be medium coarse sand. (Resistivity;69.9Ωm, Depth;1.25-9.26m, 1.25-19.8m and beyond, Spread;14-18m). The formation could be wet clay. It appears throughout the profile, at different thicknesses sand intrudes to the surface at distances of 45-48m, 50-58m, 77-82m and 83-90m. (Resistivity: 10.1-26.5Ωm, Depth: 1.25-14.0m, 3.75-19.8 and beyond, Spread:21-32m, 44-87m). This could be wet clay formation. (Resistivity: 69.9Ωm, Depth: 1.25-6.38m, 1.25-19.8m and beyond, Spread:1.0-4m, 10-14m). This layer is likely to be Clay which shows at the surface between 38-40m, 46-50m, 58-61m,73-78m and 90-95m distances along the profile.

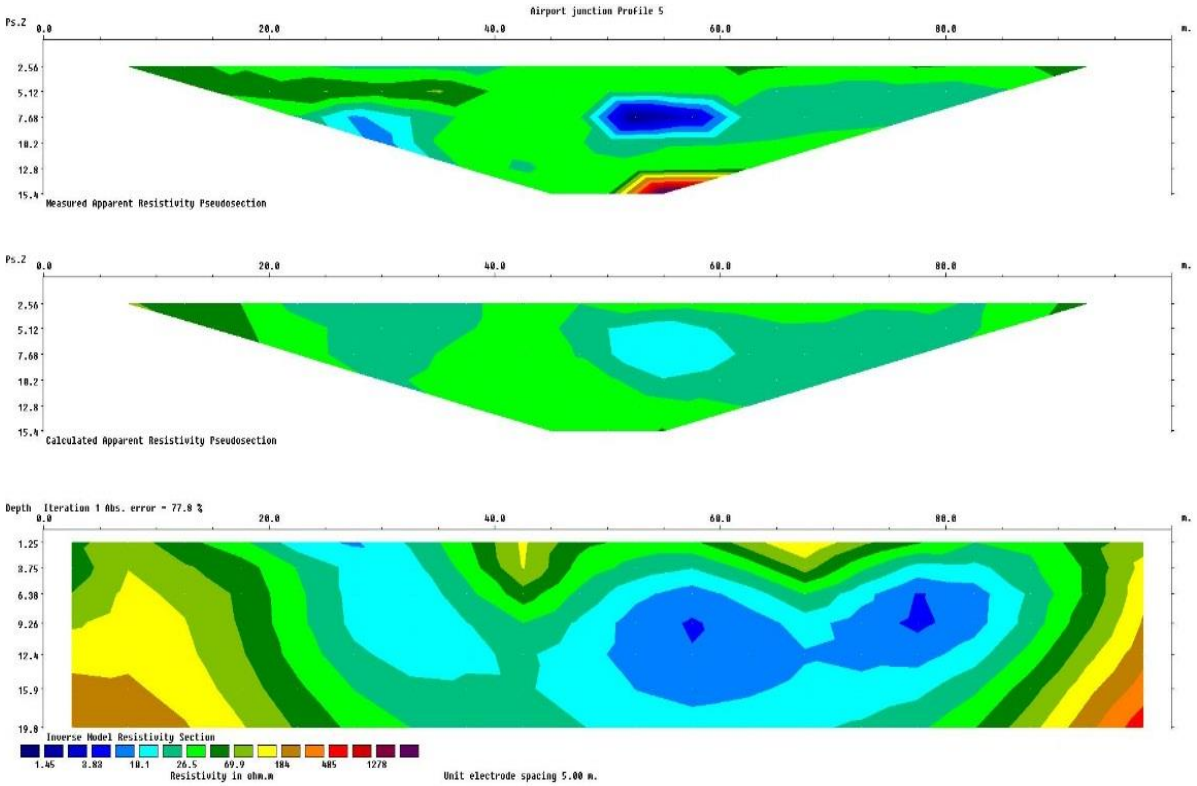

Figure 10: 2-D resistivity inversion results for profile 5

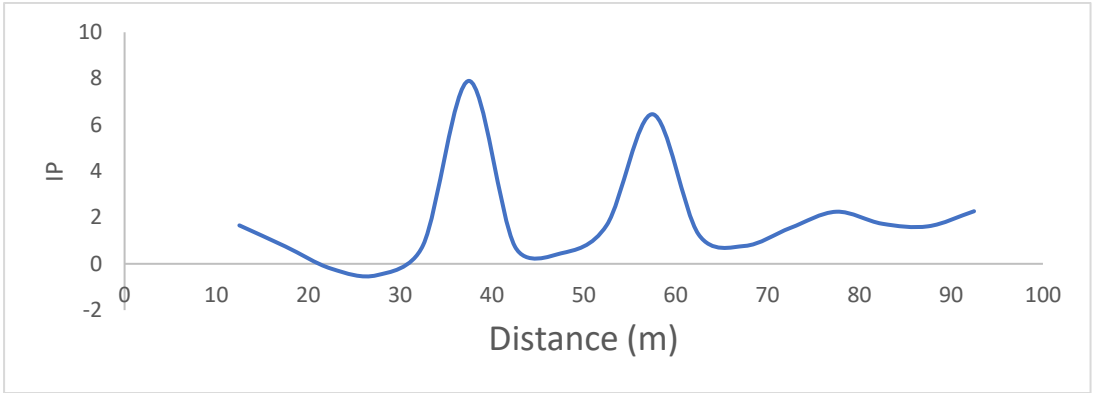

Figure 11: IPChargeability (ms) against electrode distance X(m) for profile 5

There is a low positive IP Chargeability varying between 0 – 8ms along the profile in this station (Figure 11). This represents the presence of dominant Clay bed to corroborate the observation on 2-D resistivity inversion in Fig. 10. There are zones of clayey sand and sandy clay beds of varying resistivity values of about 69.9Ωm as shown on the inverse resistivity section (Figure 10). This profile reveals resistivity ranging from 3.83 to 485Ωm, where 3.83- 69.9 is wet clay; 184 - 485Ωm is medium coarse sand which only exists at the lower ends of the base layer.

The summary of the distribution of resistivity, depth, spread and soil types encountered in the study area is shown in Table 1.

Table 1: Distribution of resistivity, depth, spread and soil type.

Profile	Resistivity /Ωm	Depth/m	Spread/m	Soil type
1	45.3-89.1	0-1.25	0-100	Topsoil
	90.0	1.25-15.9	7-100	Clayey Sand
	175.0	1.25-19.8	4-100	Fine S
	89.1	1.25-12.4	6-100	Sandy Clay
	46.0	2-10	13-40, 45-66	Wet Clay
2	9.48-44.5, 96.9-459	0-1.25	0-100	Topsoil
	96.9	2-19.8	1-30	Sandy Clay
	45.3	1.25-19.3	1-100	Wet Clay
	1.98-4.32	3.75-12.4	55-78	Fine wet Clay
	495	1.25-3.75	54-60	Medium Fine Sand
3.	46.5-89.5, 172-638	0-1.25	0-100	Topsoil
	172	2-3.75,1.25-19.8	1-100	Fine Sand
	638	6.38-17	15-25	Medium coarse Sand
	311	4-19.8	9-27	Fine Sand
	89.5	3.75-8, 5-19.8	30-81	Sandy Clay
4	20.3-61.3, 107.187	0-1.25	0-100	Topsoil
	61.5	6.38-8, 3.75-19.8	35-36, 40-53,	Clay
			68-71, 86-90	Clay
	150-187	5-19.8	1-50	Silt Fine Sand
	20.3-35.3	1.25-14	57-87	Wet Clay
	107	10-14, 3.75-19.8	1-62	Sandy Clay
	150-187	5-19	1-50	Fine Sand
Profile	Resistivity/ Ωm	Depth/m	Spread/m	Materials
5	18.1, 69.9, 184	0-1.25	0-100	Topsoil
	300	14-19.8	1-10	Medium Fine Sand
	184	10-14, 7-19	1-16	Fine Sand
	69.9	1.25-9.26,1.25-19.8	14-18, 45-48,	Wet Clay
			50-58,77-82	,,
			83-90	Wet Clay
	10.1-26.5	1.25-14,	21-32	Wet Clay
		3.75-19.8	44-87	Wet Clay
	69.9	1.25-6.38,1.25-19.8	1-4, 10-14	Clay

CONCLUSION

Resistivity in the study area varies between 1.98Ω and 835Ωm at different depths below the surface, as shown in profile 2 (Ogobiri junction) and profile 3 (Ogobiri-Tombia road).These areas comprises of sandy Clay, Wet Clay, fine Sand, Medium Coarse sand, medium fine sand at shallow depth ranging from 1.25 to 19. Low resistivity (45 - 175 Ωm), indicating Clayey sand, Fine Sand, wet Clay and sandy Clay beneath the surface was recorded at Ndu New site . This low resistivity is strongly induced by the presence of one of the tributaries of River Nun in the area. This profile 1 also recorded negative IP chargeability to indicate distribution of chargeable zones in the ground and thin chargeable zone at the surface. Profile 4, the second profile around Ogobiri- Tombia road has resistivity between 20 and 187 Ωm, having Fine sand, Wet sand, Silt fine sand Clay and Sandy Clay as materials beneath the surface at depth between 1.25 and 19.8m. At profile 5 (Airport road), resistivity decreases downward ranging between 10.1 and 300 Ωm at the top, underlain by Clay, Fine sand, medium fine sand, and wet Clay. The Induced Polarization (IP) imaging signatures corroborated these conclusions as strong, relatively, positive IP chargeability effects were observed along the profile containing clayey sand and sandy clay. In contrast, compacted clay showed low IP effects (Figures 6,8,10 and 12). Only in profile 1 (Figure 4) was the negative IP chargeability obtained throughout and this revealed the distribution of chargeable zones in the ground and could also indicate the presence of chargeable layer at the surface. It was also observed, though of very minimal extent in Profiles 2, 3 and 4. It is revealed that the resistivity changes vertically and laterally within study area, depicting the presence of sediments of varying compressions and compositions.

These results have shown that the combined geophysical methods used are of immense benefits and appropriate to characterize the subsurface strata.

REFERENCES

Abdullah, M.A. (2018). Applied Geophysics. https://www.studocu.com

Aizebeokhai, A, P., Oyeyemi, K, D., and Joel,E. S. (2016).Electrical resistivity and induce polarization imaging for groundwater exploration. Society of Exploration Geophysics (SEG) 87thAnnual Meeting https://library.seg.org/doi/10.1190/tle36020120

Alabi, A.A., Ogungbe,A.S., Adebo, B. and Lamina, O.L. (2010). Induced polarization interpretation for subsurface characterization: A case study of Obadore, Lagos State. Archives of Physics Research, 1 (3):34-43. https://www.scholarsresearchlibrary.com/archive

Allen, J.R.L.(1965).Late Quaternary Niger Delta and adjacent areas: sedimentary environment and litho facies. American Association of Petroleum Geologists Bulletin 49, 549-600. https://www.scirp.org/reference

Aristodemou, E. and Thomas-Betts,A. (2000).DC resistivity and induced polarization investigations at a waste disposal site and its environments, Journal of Applied Geophysics,44 (2-3): 275-302. https://irep.ntu.ac.uk/9195

Arjwech, R.,and Everett, M.E. (2019). Electrical resistivity tomography at construction sites in northeast Thailand with implications for building foundation design. Journal of Environmental Engineering Geophysics, 24(2):333-340. https://pubs.geoscienceworld.org/jeeg/article/24/2/333/571935

Caputo. R., Piscitelli. S., Oliveto, A., Rizzo, E., and Lapenna, V. (2003).The use of electrical tomography in active tectonics: Examples from the Tyrnavos Basin, Greece. Geophysics, 36(1-2):19-35. https://geoscienceletters.springeropen.com/articles

Chambers, J.E., Kuras, O., Meldrum, P.I., Ogilvy, R.D. and Hollands, J. (2006).Electrical resistivity tomography applied to geologic, hydro-geologic, and engineering investigations at a former waste-disposal site. Geophysics, 71(6):231-239. https://iopscience.iop.org/article/10.1088/1742-6596/1217/1/012001

Chang, P.Y., Chang. L.C., Hsu, S.Y., Tsai, J.P.. and Chen. W.F. (2017).Estimating the Hydro-geological parameters of an unconfined aquifer with the time lapse resistivity-imaging method during pumping tests: case studies at the Pengtsuo and Dajou sites. Taiwan. Journal of Applied Geophysics, 144:134-143. https://scholars.ncu.edu.tw/en/publications

Dahlin, T and Loke, M.H. (1998). Resolution of 2-D Wenner resistivity imaging as assessed by numerical modeling. Journal of Applied Geophysics, 38, 237-249. https://www.scirp.org/(S(351jmbntvnsjt1aadkozje)

Ganiyu, S.A., Badmus,B.S., Oladunjoye, M.A., Aizebeokhai, A.P., and Olurin, O.T. (2015). Delineation of Leachate Plume migration using Electrical resistivity imaging on Lapite Dumped site in Ibadan. Southwestern Nigeria. Geosciences, *5*(2); 70-80. https://www.mdpi.com/journal/geosciences

Johansson,B., Jones,S., Dahlin,T,. and Flyhammar, P. (2007). 'Comparisons of 2D- and 3D- inverted resistivity data as well as of resistivity- and IP-surveys on a landfill," in Proceedings of the 13th European Meeting of Environmental Geophysics of the Near Surface, Istanbul, Turkey. https://www.proceedings.com

Koda, E., Tkaczyk, A., Lech, M., and Osiński, P. (2017).Application of electrical resistivity data sets for the evaluation of the pollution concentration level within landfill subsoil. Applied Science 7(3):262. https://www.mdpi.com/2076-3417/7/3/262

LAYADE, G.O., ADEGOKE J.A., AND OYEWOLE, I.T.(2017).Integrated Geophysical Investigation of the Causes of Road Pavement Failure along Ibadan-Lagos Dual-Carriage, Southwestern, Nigeria. Journal of Applied Science and Environmental Management. 21 (3): 547-554. https://www.researchgate.net/publication/318557095

Nwajide, C. S. (2013). Geology of Nigeria's Sedimentary Basins. Lagos: CSS Bookshop Ltd. https://www.scirp.org/reference

Parasnins, D.S. (1986).Principles of Applied Geophysics 4th ed. London: Chapman and Hall. https://www.cambridge.org/core/journals

Short, K.C. and Stauble, A.J. (1967). Outline of Geology of Niger Delta. American Association of Petroleum Geologists Bulletin 51, 761-779. https://pubs.geoscienceworld.org/aapgbull

Telford, W. M., Geldart, L. P., & Sheriff, R. E. (1990). Applied Geophysics 2nd ed. New York: University Press, Cambridge, New York. https://www.scirp.org/reference

TerraDat Geophysical Innovations (2005).The use of shallow geophysical surveys applied to engineering and environmental ground investigations. TerraDat, UK Ltd., Cardiff https://www.terradat.co.uk/terradat-publications/

Van Schoor, M, (2002). Detection of sinkholes using 2D electrical resistivity imaging. Journal of Applied Geophysics, 50(4):393-399. https://www.sciencedirect.com/science/article/abs/pii/S0926985102001660b.

Zhang. G., Zhang, G.B., Chen, C.C., Chang, P.Y., Wang. T.P., Yen. H.Y., Dong. J.J., Ni. C.F., Chen. S.C., and Chen, C.W. (2016). Imaging rainfall infiltration processes with the time-lapse electrical resistivity imaging method. Pure Applied Geophysics, 173(6):2227-2239. https://scholars.ncu.edu.tw/zh/publications